Original Article

Ubiquitin ligase MDM2 mediates endothelial inflammation in Kawasaki disease vasculitis development

Lei Xu[1,2#], Guang-Hui Qian[1#], Liyan Zhu[3], Hong-Biao Huang[1], Cheng-Cheng Huang[1], Jie Qin[1], Yi-Ming Zheng[1], Ling Sun[1], Yan Ren[4], Yue-Yue Ding[1,5], Hai-Tao Lv[1]

[1]Department of Cardiology, Children's Hospital of Soochow University, Suzhou, China; [2]Department of Pediatric, Suzhou Municipal Hospital, The Affiliated Suzhou Hospital of Nanjing Medical University, Suzhou, China; [3]Department of Experimental Center, Medical College of Soochow University, Suzhou, China; [4]Department of Radiology, Huashan Hospital of Fudan University, Shanghai, China; [5]Ultrasonography Department, Jing'an District Centre Hospital of Shanghai, Shanghai, China

Contributions: (I) Conception and design: L Xu, HT Lv; (II) Administrative support: HT Lv, YY Ding; (III) Provision of study materials or patients: L Zhu, HB Huang, CC Huang, J Qin; (IV) Collection and assembly of data: YM Zheng, L Sun, Y Ren; (V) Data analysis and interpretation: L Xu, GH Qian; (VI) Manuscript writing: All authors; (VII) Final approval of manuscript: All authors.

[#]These authors contributed equally to this work.

Correspondence to: Hai-Tao Lv, MD. Department of Cardiology, Children's Hospital of Soochow University, Zhongnan Street, Suzhou 215000, China. Email: haitaosz@163.com; Yue-Yue Ding, MD. Department of Cardiology, Children's Hospital of Soochow University, Zhongnan Street, Suzhou 215000, China; Ultrasonography Department, Jing'an District Centre Hospital of Shanghai, 259 Xikang Road, Shanghai 200040, China. Email: dyyqd79@hotmail.com.

Background: Kawasaki disease (KD) often complicates coronary artery lesions (CALs). Despite the established significance of STAT3 signaling during the acute phase of KD and signal transducer and activator of transcription 3 (STAT3) signaling being closely related to CALs, it remains unknown whether and how STAT3 was regulated by ubiquitination during KD pathogenesis.

Methods: Bioinformatics and immunoprecipitation assays were conducted, and an E3 ligase, murine double minute 2 (MDM2) was identified as the ubiquitin ligase of STAT3. The blood samples from KD patients before and after intravenous immunoglobulin (IVIG) treatment were utilized to analyze the expression level of MDM2. Human coronary artery endothelial cells (HCAECs) and a mouse model were used to study the mechanisms of MDM2-STAT3 signaling during KD pathogenesis.

Results: The MDM2 expression level decreased while the STAT3 level and vascular endothelial growth factor A (VEGFA) level increased in KD patients with CALs and the KD mouse model. Mechanistically, MDM2 colocalized with STAT3 in HCAECs and the coronary vessels of the KD mouse model. Knocking down MDM2 caused an increased level of STAT3 protein in HCAECs, whereas MDM2 overexpression upregulated the ubiquitination level of STAT3 protein, hence leading to significantly decreased turnover of STAT3 and VEGFA.

Conclusions: MDM2 functions as a negative regulator of STAT3 signaling by promoting its ubiquitination during KD pathogenesis, thus providing a potential intervention target for KD therapy.

Keywords: Kawasaki disease (KD); murine double minute 2 (MDM2); signal transducer and activator of transcription 3 (STAT3); vascular endothelial growth factor A (VEGFA); ubiquitination

Submitted Aug 30, 2023. Accepted for publication Dec 17, 2023. Published online Feb 27, 2024.
doi: 10.21037/tp-23-459
View this article at: https://dx.doi.org/10.21037/tp-23-459

Introduction

Kawasaki disease (KD) comprises a group of clinical syndromes mainly characterized by fever, rash, and lymphadenopathy. It is a main cause of acquired cardiovascular diseases in developed countries (1,2). The main pathological features include systemic nonspecific vasculitis of small and medium arteries, especially the development of coronary artery lesions (CALs). However, the pathogenesis of KD is still unclear, although some studies have shown that the pathogenesis of KD might involve early innate immunity and acquired immunity, and it is closely related to the abnormal activation of the immune response and inflammatory cascade reaction (3-5). This immune activation results in the release of many inflammatory factors into the bloodstream, which stimulate endothelial cells to participate in the progression of CALs. Therefore, early diagnosis and treatment of KD is needed, especially for coronary artery injury, and the signaling pathways and pathogenesis of vascular endothelial inflammatory injury related to KD need to be elucidated.

The integrity of the vascular endothelium protects tissues and organs from edema and uncontrolled invasion of inflammatory cells. Several studies have shown that in addition to protein phosphorylation, ubiquitylation is an important and dynamic posttranslational modification that regulates Rho GTPases, junctional proteins, and consequently, endothelial barrier function (6). Murine double minute 2 (MDM2) is an E3 ligase, that promotes the binding of protein substrates to ubiquitin and mediates the degradation and decomposition of substrate proteins through ubiquitination. MDM2 is expressed in many human organs and cells, such as vascular endothelial cells, skeletal muscle cells, T cells, and tumor cells (7-9). It participates in various physiological and pathological processes, including the cell cycle, cell apoptosis, tumor metastasis, and angiogenesis. MDM2 inhibits T-cell activation by targeting the ubiquitination-mediated degradation of nuclear transcription factor 1 (NFAT1) (7). We found that the NFAT signaling pathway is involved in immune damage in patients with KD in another study (10). Therefore, we hypothesized that the ubiquitination of proteins associated with MDM2 plays a crucial role in KD.

Furthermore, according to our previous research, signal transducer and activator of transcription 3 (STAT3) participates in vascular endothelial inflammatory injury in patients with KD by regulating adhesion molecules and E-selectin on the surface of endothelial cells (11). Moreover, STAT3 was shown to participate in heart development by regulating various cardiovascular diseases including ischemic heart injury, cardiac fibrosis, and the occurrence and development of inflammatory reactions in tumors (12,13). Abnormal STAT3 signaling can promote angiogenesis and change vascular permeability by regulating the expression of its downstream target gene *VEGF* (vascular endothelial growth factor) (14,15). Notably, Lipopolysaccharide (LPS)-activated STAT3 can increase the production of VEGF and stimulate endothelial cell migration and tubule formation, which in turn can promote angiogenesis (16,17). The STAT3 activation involves its phosphorylation and nuclear transport when stimulated by various cytokines or other stimuli. More specifically, the interaction between the phosphorylated SH2 domain and the Tyr705 site generate homologous dimers of phosphorylated STAT3, which are transferred from the cytoplasm to the nucleus, where they promote the transcription of downstream target genes (16,18). Except for phosphorylation, the ubiquitin-proteasome system (UPS) also regulates the stability of STAT3. Tumor necrosis factor receptor-associated factor 6 (TRAF6) can mediate the ubiquitination of lysine-63 in the SH2 region of STAT3, thus activating the STAT3 signaling pathway through ubiquitin ligases (19,20).

The VEGF family mainly comprises placental growth factor (PIGF) and VEGF-A, B, C, D, and E. Among the six members, VEGFA strongly influences vascular endothelial function and vascular permeability. It

Highlight box

Key findings

- Murine double minute 2 (MDM2) functions as a negative regulator of STAT3 signaling by regulating its ubiquitination during Kawasaki disease (KD) pathogenesis.

What is known and what is new?

- Signal transducer and activator of transcription 3 (STAT3) signaling has been shown to be involved in the acute phase of KD and is closely related to coronary artery lesions.
- We first elucidated the relationship between MDM2 and STAT3 in the pathogenesis of KD, in which MDM2 acts as a negative regulator of STAT3 signaling by regulating its ubiquitination during inflammatory responses in KD.

What is the implication, and what should change now?

- The downregulation of MDM2 in the acute stage of KD can induce a reduction in ubiquitin-mediated degradation of STAT3, which in turn can lead to the upregulation of vascular endothelial growth factor A. These changes might be associated with the pathogenesis of Kawasaki disease.

regulates the formation of blood vessels in tumor tissues, where it activates static endothelial cells, promotes cell proliferation and migration, and eventually increases vascular permeability (21). The expression of VEGFA in peripheral blood mononuclear cells (PBMCs) and neutrophils of children with KD was determined by Western blotting, and the VEGFA level in children with KD was found to be significantly higher. The results of an enzyme-linked immunosorbent assay (ELISA) showed high levels of VEGFA in the plasma of KD patients during the acute stage. VEGFA, along with CALs, was found to be an important risk factor for KD (22-24). In this study, we hypothesized that MDM2 might target STAT3 and further activate VEGFA, which might participate in vascular endothelial inflammatory injury in patients with KD. We present this article in accordance with the MDAR and ARRIVE reporting checklists (available at https://tp.amegroups.com/article/view/10.21037/tp-23-459/rc).

Methods

Study subjects

This study was approved by the Ethics Committee of the Children's Hospital of Soochow University (reference number 2021CS013), and all parents of the participants provided informed consent before the participants were enrolled. This study was conducted following the guidelines of the Declaration of Helsinki (as revised in 2013). Patients diagnosed with KD according to the diagnostic criteria established by the American Heart Association guidelines in 2017 were recruited from the Children's Hospital of Soochow University between October 2018 and May 2019. We classified the KD patients with CALs (KD-CALs) (n=45) into two phases. The acute phase was defined as the febrile period before intravenous immunoglobulin (IVIG) administration, and the subacute phase was defined as the afebrile period after treatment with IVIG for three days. CALs were defined based on the internal lumen diameter of the proximal and middle segments of the left main coronary artery (LMCA), the left anterior descending artery (LAD), the left circumflex coronary artery (LCX), and the right coronary artery (RCA), following a criterion of standard Z-value ≥2.0. The Z-score was calculated based on the data including weight, height, age, gender and coronary artery diameter (25). Patients in the control group underwent regular health examinations and had no infection. The criteria for the fever group were that the main clinical manifestation was fever (axillary temperature >37.5 ℃ and duration of fever ≥3 days) with bacterial infections, and routine blood tests showed a high level of white blood cells and/or C-reactive protein (CRP).

The whole blood sample (2 mL) was collected in a tube containing EDTA. The serum and PBMCs were isolated and stored at −80 ℃ for further use. The samples were not frozen and thawed repeatedly.

Preparation of the Candida albicans water-soluble fraction (CAWS)

Candida albicans (NBRC:1385) was purchased from the Osaka Institute of Biology, Japan. To make the CAWS, *C. albicans* was dissolved in sterilized water, and an appropriate quantity of the mixture was added to Shahler's culture medium under constant shaking at 1,600 rpm at 27 ℃ overnight. The following day, 1 mL of the culture medium was added to 1 L of sterilized nutrient solution and shaken at 1,600 rpm at 27 ℃ for 24 h. Next, 500 mL of anhydrous ethanol was added, the solution was incubated at 4 ℃ overnight, and then, it was centrifuged. The pellet was collected, rinsed, stirred with double distilled water for 2 h, and then centrifuged at 4 ℃ and 9,000 rpm for 15 min. The supernatant was retained, and an equal volume of anhydrous ethanol was added, incubated at 4 ℃ overnight, and then centrifuged at 4 ℃ and 9,000 rpm for 15 min. The precipitate was collected using acetone and dried in a biological cabinet. The precipitate was dissolved in phosphate-buffered saline (PBS) to a final concentration of 100 mg/mL.

CAWS-induced mouse model

We purchased C57BL/6 specific pathogen-free male mice (n=25; four weeks old) from Shanghai Linchang Biological Technology Co., Ltd. (Shanghai, China). The mice were housed in standard experimental cages and reared under controlled conditions (temperature =25±2 ℃; humidity =50%±5%). The mice were divided randomly into five groups (n=5 mice per group), which included a normal control group (WT), a PBS group, and three CAWS groups, in which the mice were intraperitoneally injected with CAWS (4 mg/mouse) for five consecutive days (26). After one to 14 days after the last CAWS injection, we collected the hearts of the mice. All mice were killed by CO_2 suffocation. The animal experiments were conducted following the National Institutes of Health Guide for the

Care and Use of Laboratory Animals. The Animal Care and Use Committee of Soochow University approved the experiments (approval number: SUDA20220906A01). The protocols used in the study were prepared before the study without registration.

Cell culture and treatment

Human coronary artery endothelial cells (HCAECs) were purchased from Shanghai Biological Cell Bank (Shanghai, China). The HCAECs were cultured using Roswell Park Memorial Institute (RPMI)-1640 Medium (Gibco, Grand Island, NY, USA) containing 1% penicillin/streptomycin and 10% fetal bovine serum in a humidified atmosphere with 5% CO_2 at 37 ℃. Then, the HCAECs were seeded in a six-well plate at 3×10^5 cells/mL. The HCAECs were stimulated with 40 ng/mL tumor necrosis factor alpha (TNF-α) for approximately 4 h. Then, the total mRNA and proteins were extracted from the cells. Finally, quantitative reverse transcription PCR (qRT-PCR) and Western blotting analyses were performed to determine the levels of MDM2, STAT3, and VEGFA expression.

Viral infection in vitro

The overexpression and knockdown lentiviruses were purchased from Shanghai Genechem Co., Ltd. (Shanghai, China). Transfection was performed after the cells reached 70% confluence. The cells were divided into four groups, including the Control group (RPMI-1640 Complete Medium), Mock group (RPMI-1640 Complete Medium + virus), A group (RPMI-1640 Complete Medium+ virus + infection enhancement solution A), and P group (RPMI-1640 Complete Medium + virus + infection enhancement solution P). RPMI-1640 Complete Medium at the corresponding volume was added according to the multiplicity of infection (MOI) = 1 [1×10^6 transduction units (TU)/mL], 10 (1×10^7 TU/mL), and 100 (1×10^8 TU/mL). Next, the viruses and the corresponding infection enhancement solution A/P were mixed and cultured. The RPMI-1640 Complete Medium was replaced 12 h after infection. After 72 h of infection, a fluorescence microscope was used to observe the infection intensity and assess the cell status.

Short interfering RNAs (siRNAs) targeting *MDM2*:

- MDM2-RNAi (62913–1) CTCAGCCATCAACTT CTAGTA.
- MDM2-RNAi (62914–1) GATTCCAGAGAGTCA TGTGTT.
- MDM2-RNAi (61915–1) CTTTGGTAGTGG AATAGTGAA.

Short interfering RNAs (siRNAs) targeting *STAT3*:

- STAT3-RNAi (82767–1) GCACAATCTACGAA GAATCAA.
- STAT3-RNAi (82768–1) CTCAGAGGATCCCG GAAATTT.
- STAT3-RNAi (82769–1) GGCGTCCAGTTCAC TACTAAA.

Western blotting assay

An equivalent amount of proteins was used to perform SDS-PAGE, and then, the proteins were transferred onto polyvinylidene fluoride (PVDF) membranes (Millipore, Billerica, MA, USA). The PVDF membranes were blocked with either 5% nonfat milk or 5% bovine serum albumin (BSA) for 0.5 h at 27 ℃ and then incubated with the corresponding primary antibodies (Abs) at 4 ℃ overnight. After washing thrice with PBST (1× PBS and Tween 20), the membranes were incubated with secondary Abs [horseradish peroxidase (HRP)-conjugated goat anti-rabbit or goat anti-mouse antibodies (Servicebio, Wuhan, China)] in 5% nonfat milk for 1 h. After washing thrice with TBST, the immunoreactive proteins on the membranes were visualized using an ECL luminescent liquid. Image-pro plus software (Media Cybernetics, Rockville, MD, USA) was used to analyze the gray values of the bands after imaging in an Amersham Imager 600 developer (Amersham, UK). The antibodies used along with the indicated dilutions were as follows: anti-MDM2 (Cell Signaling Technology, Danvers, MA, USA; #86934S, 1:1,000), anti-STAT3 (Cell Signaling Technology; #9139S, 1:1,000), anti-glyceraldehyde-3-phosphate dehydrogenase (GAPDH) (Abcam, Cambridge, MA, USA; ab181602, 1:1,000), anti-Flag (Sigma, St. Louis, MO, USA; F7425, 1:5,000), and ubiquitin (Santa Cruz Biotechnology, Santa Cruz, CA, USA; sc-8017, 1:500).

qRT-PCR

Initially, total mRNA was extracted from cells and tissues and reverse transcribed to complementary DNA (cDNA). Then, cDNA was quantified via quantitative real-time PCR (qPCR) analysis using a SYBR Green kit (Selleck Chemicals, Houston, TX, USA). The relative gene expression levels were calculated using the change in the cycle threshold ($2^{-\Delta\Delta CT}$) method (27). GAPDH was used as an endogenous

control. The ΔΔCT method was used to analyze the relative gene expression data. The results are obtained from three independent experiments and presented as the mean ± SD.

The sequences of primers used were as follows.

Human (H)-*GAPDH*:

- Forward: ACCCACTCCTCCACCTTTGA.
- Reverse: CTGTTGCTGTAGCCAAATTCGT.

H-*MDM2*:

- Forward: CTTCTAGGAGATTTGTTTGGCG.
- Reverse: ATGTACCTGAGTCCGATGATTC.

H-*STAT3*:

- Forward: TCGGCTAGAAAACTGGATAACG.
- Reverse: TGCAACTCCAGTTTCTTAA.

H-*IL6*:

- Forward: CACTGGTCTTTTGGAGTTTGAG.
- Reverse: GGACTTTTGACTCATCTGCAC.

Mouse (M)-*Gapdh*:

- Forward: AGGTCGGTGTGAACGGATTTG.
- Reverse: GGGGTCGTTGATGGCAACA.

M-*VEGFA*:

- Forward: TCTGGGCTCTTCTCGCT.
- Reverse: CCTTCTCTTCCTCCCCTCT.

ELISA

The level of VEGFA in the serum of patients was measured using specific ELISA kits (Shenzhen Dakewe Biological Engineering Co., Ltd., Shenzhen, China) following the manufacturer's instructions.

Immunoprecipitation (IP) assay

The cells were harvested in lysis buffer containing 150 mM NaCl, 20 mM Tris-HCl (pH 7.4), 1% Nonidet P-40, 0.5 mM EDTA, phenylmethylsulfonyl fluoride (PMSF) (50 μg/mL), and protease inhibitor mixtures (Sigma). While examining protein ubiquitination, radioimmunoprecipitation assay (RIPA) lysis buffer (Beyotime, Jiangsu, China) was used, and N-ethylmaleimide (10 mM) was added to the lysis buffer. The cell lysates were incubated with specific Abs under constant rotation at 4 ℃ overnight. Protein agarose beads (Millipore; 16–266) were first washed twice and then added to the samples and incubated overnight. The mixture was incubated for 4–6 h on a rotor at 4 ℃. After washing thrice with wash buffer containing 150 mM NaCl, the immunoprecipitated proteins were analyzed by Western blotting analysis.

In Silico method

We used UbiBrowser (http://ubibrowser.ncpsb.org) to predict the E3 ligases.

Statistical analysis

All experiments were repeated thrice. GraphPad Prism 8 (GraphPad Inc., La Jolla, CA, USA) and SPSS 22.0 (IBM Corp., Armonk, NY, USA) were used to analyze the data, and Image J (NIH, Bethesda, MD, USA) software was used to measure the gray value of WB. The Shapiro-Wilk test was conducted to determine whether the data followed a normal distribution. The mean ± standard deviation ($\overline{x}$ ± SD) represented the measurement data. The differences in the data between any two groups were analyzed using the two-tailed unpaired Student's *t*-test. The differences in the data among multiple groups were compared by performing one-way analysis of variance (ANOVA) univariate variance. Correlations between groups were analyzed using Spearman's correlation method. All results were considered to be statistically significant at $P<0.05$.

Results

Clinical features

There were no differences in sex, age or weight between the groups of patients and controls ($P>0.05$). The information of the three groups included in the study is shown in *Table 1*. The information of the patients with KD-CALs is shown in *Table 2*.

The MDM2 mRNA expression level decreased while the STAT3 level increased in PBMCs of KD patients with CAL

We used UbiBrowser (http://ubibrowser.ncpsb.org) to examine the putative E3 ligases that can ubiquitinate STAT3. In the network view, a node was placed in the center of the canvas showing the putative substrates, which were surrounded by nodes that revealed predicted E3 ligases. The node colors and characters denote the E3 ligase type. The edge width and node size represented the confidence score. In the confidence mode, the width of the edge and the size of the node were positively correlated with the UbiBrowser score. The correlation between STAT3 and MDM2 was the most significant (*Figure 1A*). To verify the reliability of this correlation, we evaluated the

Table 1 The characteristic features of KD-CALs, fever, and normal control groups

Characteristics	KD-CALs (n=45)	Fever (n=45)	Control (n=45)	P
Sex (male/female)	30/15	30/15	33/12	0.737
Age (months)	24.40±14.87	29.67±19.04	30.50±16.14	0.087
Weight (kg)	12.87±3.58	13.65±4.9	14.32±3.36	0.232
IVIG-resistance (+/–)	0/45	ND	ND	ND
WBC count ($\times10^9$/L)	16.4±6.03	9.36±6.14	9.12±2.45	<0.001
Hgb (g/L)	106.47±9.06	118.47±13.30	122.46±10.12	<0.001
Platelet count ($\times10^9$/L)	436.07±121.29	302.09±110.53	329.11±85.91	<0.001
CRP (mg/L)	84.24±58.16	31.06±45.54	0.62±1.83	<0.001

Data are presented as mean ± standard deviation or n/n. KD-CALs, Kawasaki disease with coronary arterial lesions; IVIG, intravenous immunoglobulin; ND, no data; WBC, white blood cell; Hgb, the mean hemoglobin concentration normalized; CRP, C-creative protein.

Table 2 The laboratory data of KD-CALs patients before and after using IVIG

Laboratory findings	KD-CALs	
	–IVIG	+IVIG
WBC count ($\times10^9$/L)	16.4±6.03	9.19±2.90
Hgb (g/L)	106.47±9.06	107.73±10.98
Platelet count ($\times10^9$/L)	436.07±121.29	487.89±143.45
CRP (mg/L)	84.24±58.16	7.26±10.32
ESR (mm/L)	35.79±24.49	27.09±20.38
ALT (U/L)	59.3±75.22	31.12±27.78
AST (U/L)	45.48±38.07	45.79±22.37
LDH (U/L)	191.02±128.86	322.87±84.27
ALB (g/L)	37.87±3.77	35.9±3.18

Data are presented as mean ± standard deviation. KD-CALs, Kawasaki disease with coronary arterial lesions; IVIG, intravenous immunoglobulin; WBC, white blood cell; CRP, C-creative protein; ESR, erythrocyte sedimentation rate; ALT, alanine aminotransferase, AST, aspartate aminotransferase; LDH, lactate dehydrogenase; ALB, albumin.

level of expression of the *MDM2* and *STAT3* mRNAs in PBMCs from patients with KD. The level of *STAT3* mRNA was higher, but the level of *MDM2* mRNA was lower in all patients with KD, in the acute stage and the subacute stage than in the respective levels in the normal and fever groups. The increase and decrease in the mRNA levels were more prominent in patients in the acute stage of KD than those in the other stages or groups (*Figure 1B*,*1C*). The results of Spearman's correlation analysis showed that the mRNA levels of *MDM2* and *STAT3* in KD were significantly and negatively correlated (r_s=–0.446, P<0.001) (*Figure 1D*). However, the correlation between *MDM2* and *STAT3* was not significant in the other groups (*Figure 1E*,*1F*). We also found that the VEGFA protein level in the KD group was higher than that in the control and fever groups (*Figure 1G*).

The expression levels of MDM2 and STAT3 were negatively correlated in the KD mouse model

To examine the role of MDM2 and STAT3 in KD, we constructed a mouse model of immune vasculitis via intraperitoneal injection of CAWS. We found infiltration of inflammatory cells around cardiac vessels in mice on day

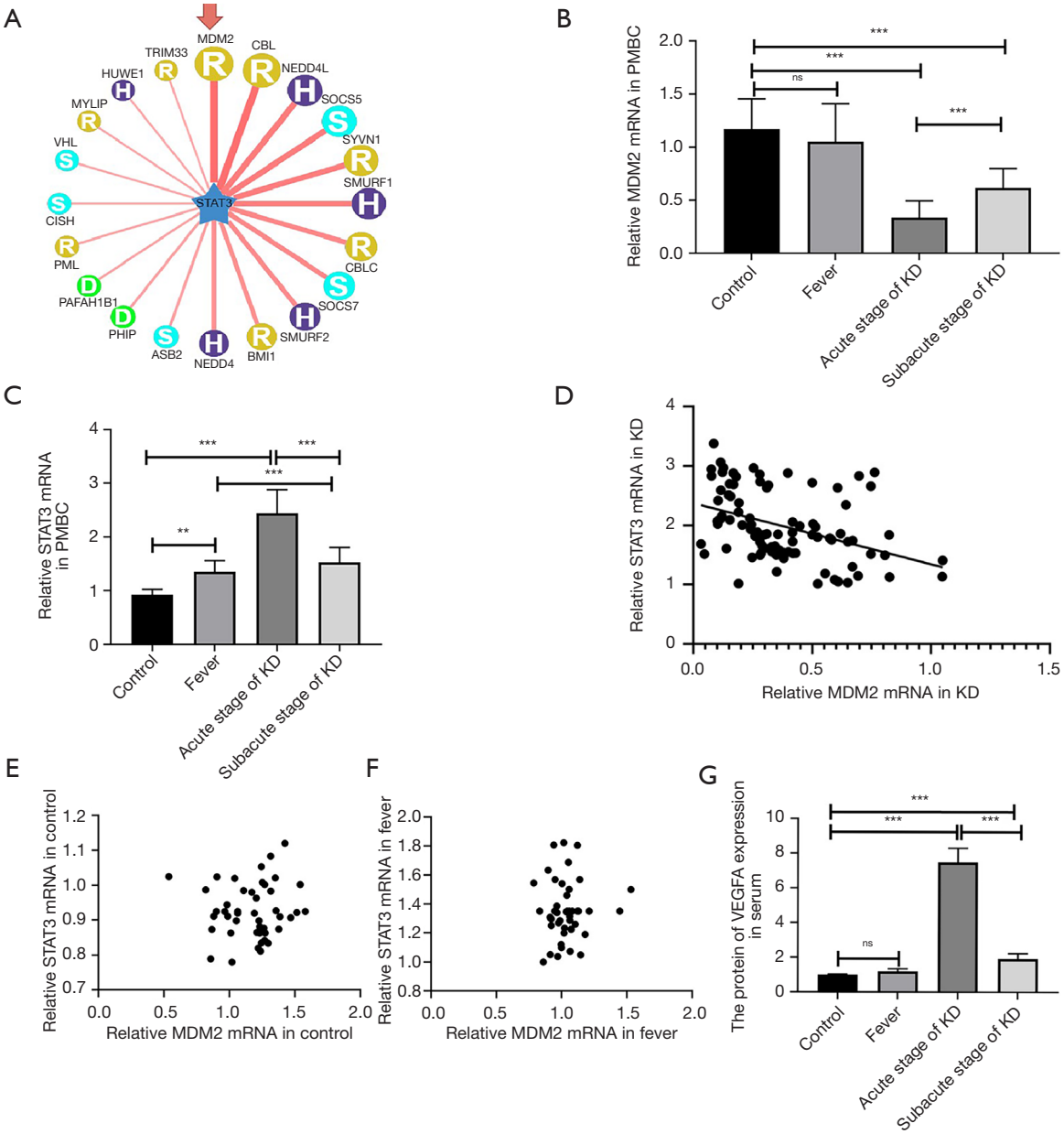

Figure 1 MDM2 was correlated with STAT3 in patients with KD. (A) A network figure showing a significant correlation between STAT3 and MDM2 (as indicated by the arrow). (B) qRT-PCR analysis was performed to determine the level of *MDM2* mRNA in the KD acute stage group, the KD subacute stage group, the normal control group, and the fever control group (n=45 individuals per group). The level of *MDM2* mRNA decreased more prominently in the KD acute stage group than in the other groups. (C) A qRT-PCR analysis showed that the *STAT3* mRNA level increased in the PBMCs from the four groups; the increase was more prominent in the KD acute stage group than in the other groups. (D) Spearman's correlation analysis showed a negative correlation between *MDM2* and *STAT3* mRNA levels in KD (r_s=–0.446, P<0.001). (E) The mRNA levels of *MDM2* and *STAT3* in the control group were not correlated (r_s=0.16, P=0.944). (F) The mRNA levels of *MDM2* and *STAT3* in the fever group were not correlated (r_s=0.04, P=0.816). (G) The ELISA results showed that the level of VEGFA in the serum from patients in the acute stage of KD increased more than that in the serum from the patients in the other groups. ***, P<0.001; **, P<0.01; ns, no significance. KD, Kawasaki disease; MDM2, murine double minute 2; PBMC, peripheral blood mononuclear cell; STAT3, signal transducer and activator of transcription 3; VEGFA, vascular endothelial growth factor A; qRT-PCR, quantitative reverse transcription polymerase chain reaction.

14, which indicated that the mouse model was constructed (*Figure 2A*). On day 7, we found that the MDM2 protein level decreased significantly, and the STAT3 level increased in the heart tissue of the mice with vasculitis (*Figure 2B,2C*). Additionally, the mRNA level of *VEGFA* began to increase in the heart tissue of the mice with vasculitis on day 7 (*Figure 2D*). To confirm our findings, we evaluated the expression of MDM2 and STAT3 in the acute stage of the heart tissues of mice in the PBS and CAWS groups under an immunofluorescence microscope. The results showed that the MDM2 fluorescence intensity was lower and the STAT3 fluorescence intensity was higher in the CAWS group than in the PBS group, and both were expressed in heart tissues and vessels (*Figure 2E,2F*). Altogether, these results resemble those obtained from the clinical samples, STAT3 and MDM2 were correlated in the mice from the KD group.

Co-localization of MDM2 with STAT3 in HCAECs

We stimulated HCAECs with TNF-α to construct a vascular inflammatory damage model of KD. We treated HCAECs with different concentrations of TNF-α and at different times to find the best time and dose. We found that treatment of HCAECs with 40 ng/mL TNF-α for approximately 4 h induced the most prominent inflammatory response (*Figure 3A,3B*). The MDM2 protein level decreased significantly, and the STAT3 protein level increased after HCAECs were treated with TNF-α (40 ng/mL) for 4 h (*Figure 3C,3D*). The *VEGFA* mRNA level increased after HCAECs were treated with TNF-α (40 ng/mL) for 4 h (*Figure 3E*). These results indicated that MDM2, STAT3, and VEGFA were involved in vascular endothelial inflammation. Using a confocal microscope, we observed that MDM2 and STAT3 were colocalized and increased after 4 h of TNF-α stimulation in cells, especially in the nucleus (*Figure 3F,3G*).

MDM2 negatively regulated STAT3 expression levels in vitro

To determine the regulatory mode of MDM2 on STAT3, we constructed lentiviruses that could downregulate the expression of *MDM2* (sh-MDM2). The lentiviruses were transfected into HCAECs at MOIs of 1, 10, and 100 at 72 h after transfection. The fluorescence intensity of the cells was most prominent when the MOI was 100, as determined by a fluorescence microscope (*Figure 4A*).

We constructed and transfected viruses that expressed three different short hairpin RNA (shRNA) targeting *MDM2* (sh-MDM2) into HCAECs. The virus construct seq-62915 had the best interference efficiency and was used for subsequent knockdown experiments (*Figure 4B*). When seq-62915 was transfected into HCAECs, the endogenous STAT3 protein level increased significantly (*Figure 4C,4D*). The *VEGFA* mRNA level increased significantly in the sh-MDM2 group (*Figure 4E*). We constructed lentiviruses that could overexpress *MDM2* (LV-flag-MDM2) and they were transfected into HCAECs (*Figure 4F*). In contrast, the STAT3 protein level and the *VEGFA* mRNA level decreased significantly after LV-flag-MDM2 was transfected into HCAECs (*Figure 4G-4I*).

MDM2 regulated STAT3 ubiquitination level and led to changes in VEGFA signaling in HCAECs

As we found a negative regulatory relationship between MDM2 and STAT3 in the *in vitro* cell model and *in vivo* mouse model, we hypothesized that MDM2 might regulate the stability of STAT3 through the ubiquitination of STAT3. To test this hypothesis, TNF-α (40 ng/mL) was used to treat HCAECs for 4 h, and an *in vitro* cell model was developed. In these cells, MDM2 and STAT3 in HCAECs were reciprocally immunoprecipitated (*Figure 5A*). When LV-Flag-MDM2 lentiviruses were transfected into HCAECs and treated for 6 h with the proteasome inhibitor MG132 (20 μM) after 72 h of transfection, we found that STAT3 ubiquitination increased significantly. The cell extracts were immunoprecipitated with anti-Ub antibodies, and the input proteins were immunoblotted with antibodies against FLAG and GAPDH (*Figure 5B*).

To confirm that STAT3 can regulate VEGF and activate it, we constructed and transfected viruses expressing three different shRNAs targeting *STAT3* (sh-STAT3) into HCAECs. The lentiviruses were transfected into HCAECs at MOIs of 1, 10, and 100 at 72 h after transfection. The fluorescence intensity of the cells was most prominent when the MOI was 100, as determined by a fluorescence microscope (*Figure 6A*). The virus constructed seq-82769 had the best interference efficiency (*Figure 6B,6C*). When we transfected seq-82769 lentiviruses into HCAECs, the expression of *VEGFA* mRNA decreased significantly (*Figure 6D*).

Discussion

The most serious complication of KD is coronary artery

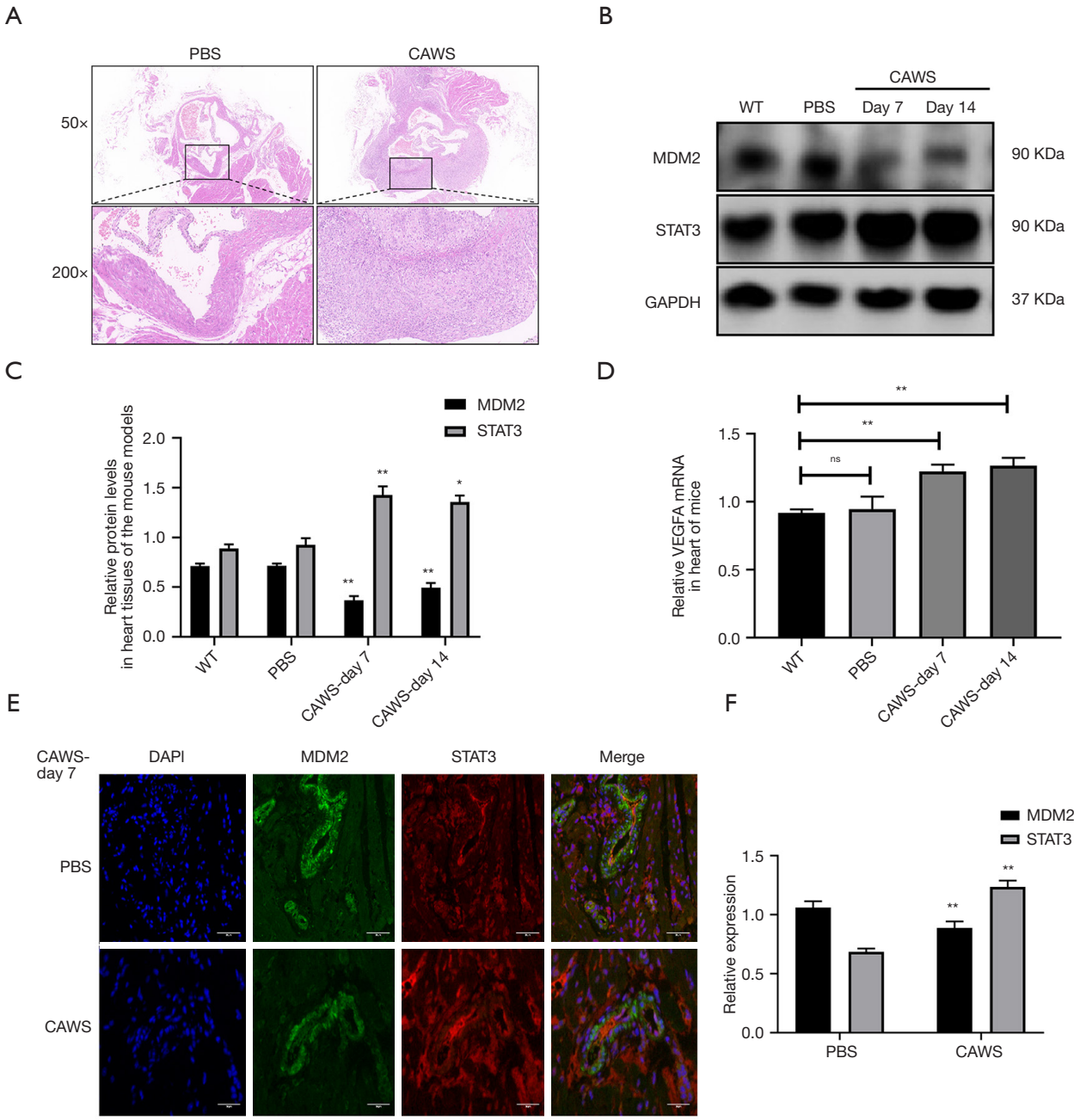

Figure 2 MDM2 was correlated with STAT3 in mice. (A) Hematoxylin and eosin staining was performed to visualize inflammatory cell infiltration around the cardiac vessels of KD in the PBS/CAWS-induced mouse model on the 14th day. Scale bars: 200 μm (50×) and 10 μm (200×). (B) Western blotting analysis was performed to determine the MDM2 and STAT3 protein levels in heart tissues of the CAWS-induced model mice on days 7 and 14. (C) Image J software was used to analyze the MDM2 and STAT3 protein levels in the heart tissues of the model mice on days 7 and 14. (D) The mRNA levels of *VEGFA* in heart tissues of CAWS-induced model mice on days 7 and 14. (E and F) Immunofluorescence staining analysis of MDM2 (green) and STAT3 (red) fluorescence intensity in the heart tissues of the PBS/CAWS-induced model mice on day 7. The nuclei were stained with DAPI in all images. Scale bars: 50 μm. **, P<0.01; *, P<0.05; ns, no significance. PBS, phosphate-buffered saline; CAWS, *Candida albicans* water-soluble fraction; WT, wildtype; KD, Kawasaki disease; MDM2, Murine double minute 2; STAT3, signal transducer and activator of transcription 3; VEGFA, vascular endothelial growth factor A.

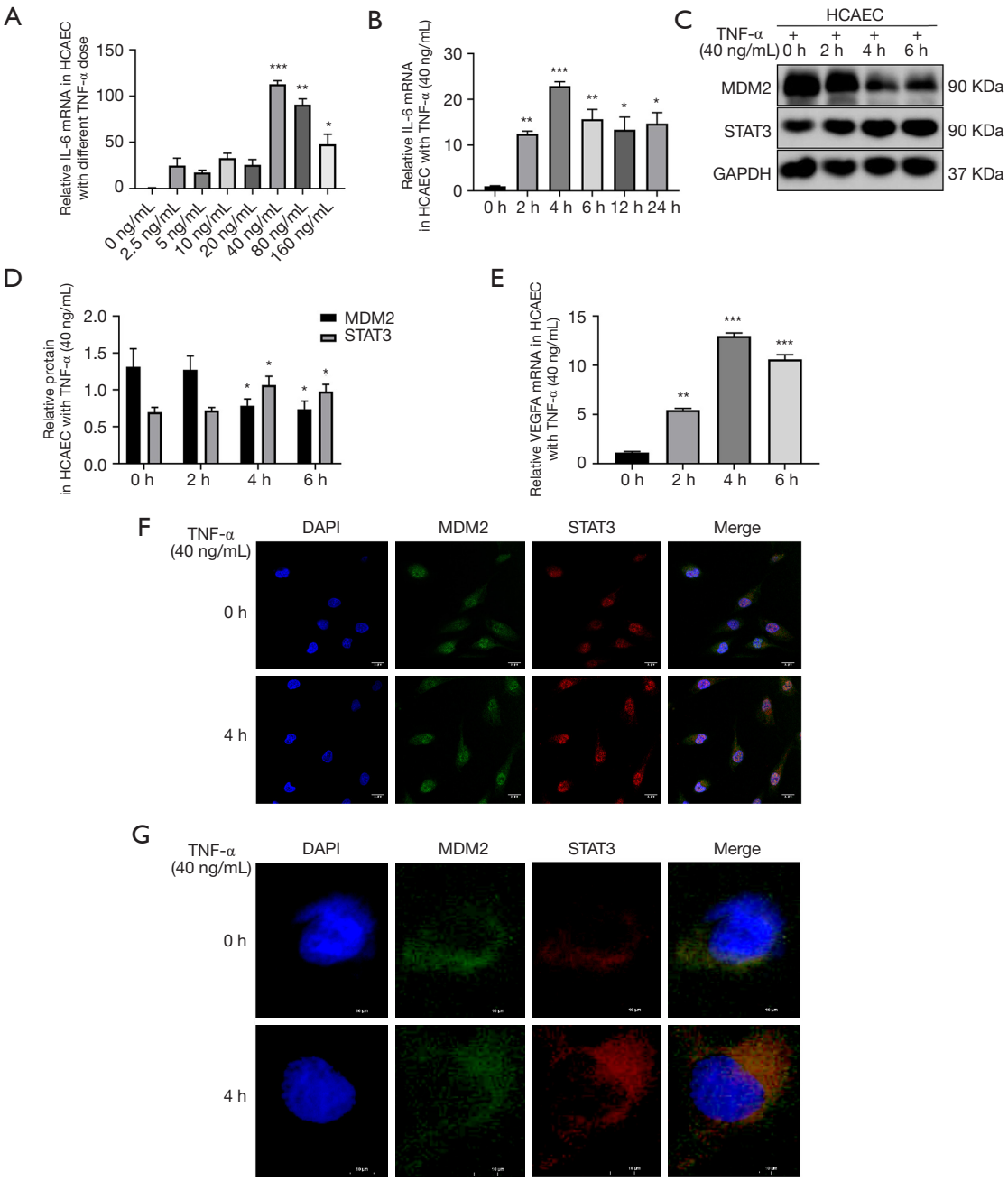

Figure 3 MDM2 was correlated with STAT3 *in vitro*. (A) qRT-PCR analysis of *IL6* mRNA levels in HCAECs stimulated with different concentrations of TNF-α (0, 2.5, 5, 10, 20, 40, 80, and 160 ng/mL) for 4 h. (B) qRT-PCR analysis of *IL6* mRNA levels in HCAECs stimulated with TNF-α (40 ng/mL) for different durations (0, 2, 4, 6, 12, and 24 h). (C) The results of the Western blotting analysis showed the MDM2 and STAT3 protein levels in HCAECs stimulated with TNF-α (40 ng/mL) in culture for 2, 4 and 6 h. (D) The expression levels of MDM2 and STAT3 were quantified by densitometry via Image J, and the level of MDM2 and STAT3 were analyzed. (E) qRT-PCR analysis was performed to determine *VEGFA* mRNA levels in HCAECs treated with TNF-α (40 ng/mL) in culture for 2, 4 6 h. (F,G) Confocal microscopy analysis of the colocalization of MDM2 (green) and STAT3 (red) was performed in HCAECs treated with TNF-α (40 ng/mL) for 4 h. Scale bars: 20 and 10 μm. ***, P<0.001; **, P<0.01, and *, P<0.05. HCAECs, human coronary artery endothelial cells; TNF-α, tumor necrosis factor α; IL-6, interleukin 6; MDM2, murine double minute 2; STAT3, signal transducer and activator of transcription 3; VEGFA, vascular endothelial growth factor A; DAPI, 4',6-diamidino-2-phenylindole; qRT-PCR, quantitative reverse transcription polymerase chain reaction.

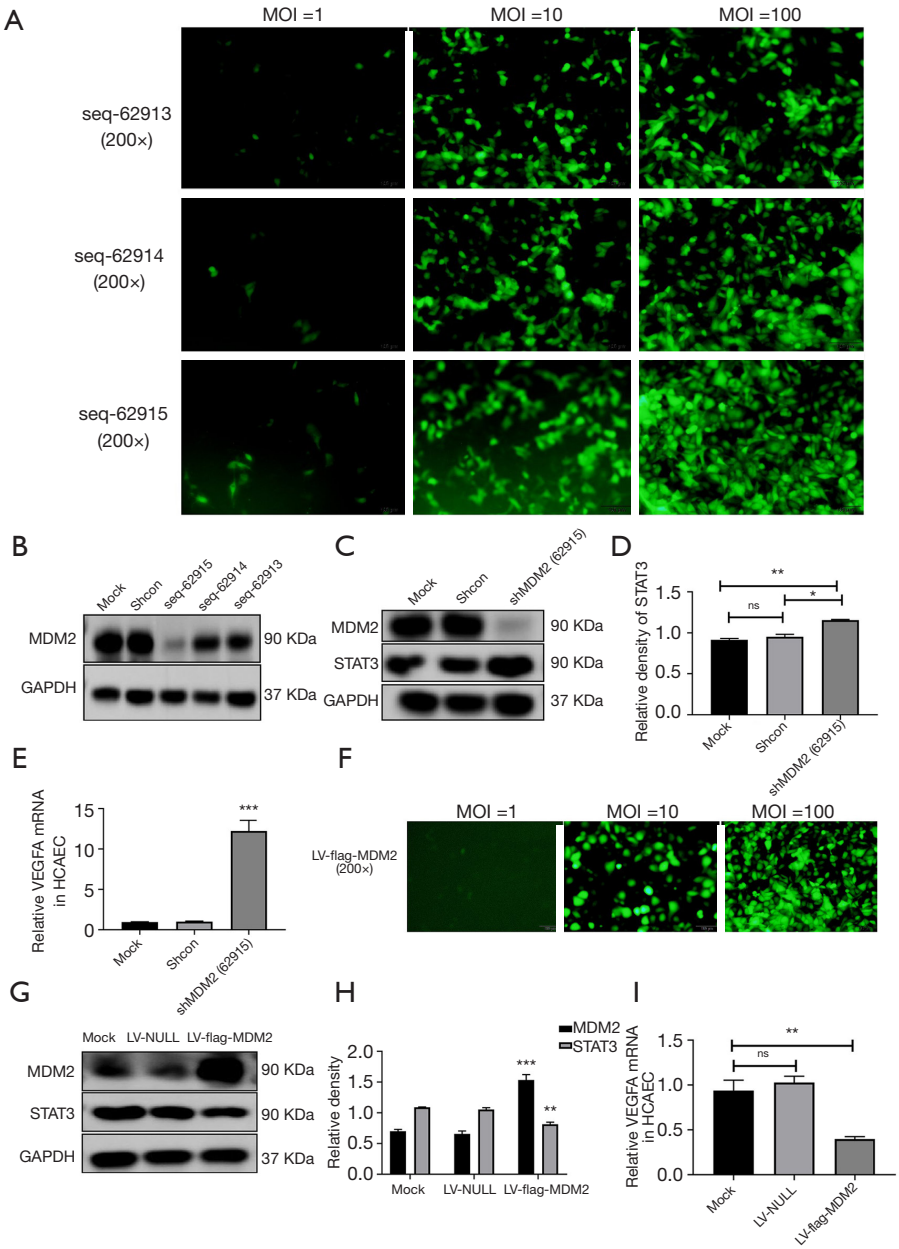

Figure 4 MDM2 targeted and regulated STAT3 *in vitro*. (A) The lentivirus used to downregulate *MDM2* expression (sh-MDM2) was transfected into HCAECs at MOIs of 1, 10, and 100 at 72 h after transfection. The fluorescence intensity of the cells was observed under a fluorescence microscope (green fluorescent protein marker). (B) Western blotting analysis of proteins obtained from HCAECs transfected with viruses encoding three different sequences that interfered with the expression of *MDM2*. (C) A Western blotting analysis was performed to determine the STAT3 levels in HCAECs transfected with MDM2-interfering viruses (sh-MDM2). (D) Image J software was used to analyze the MDM2 and STAT3 levels in (C). (E) qRT-PCR analysis was performed to determine the *VEGFA* mRNA levels in HCAECs transfected with *MDM2*-interfering viruses (sh-MDM2). (F) The lentivirus used to overexpress *MDM2* (LV-flag-MDM2) was transfected into HCAECs at MOIs of 1, 10, and 100 at 72 h after transfection. The fluorescence intensity of the cells was observed under a fluorescence microscope (green fluorescent protein marker). (G) A Western blotting analysis was performed to determine the STAT3 levels in HCAECs transfected with LV-flag-MDM2. (H) The Image J software was used to analyze MDM2 and STAT3 levels in (G). (I) A qRT-PCR analysis was performed to determine the *VEGFA* mRNA levels in HCAECs transfected with LV-flag-MDM2. ***, P<0.001; **, P<0.01, and *, P<0.05; ns, no significance. MOI, multiplicity of infection; MDM2, murine double minute 2; STAT3, signal transducer and activator of transcription 3; VEGFA, vascular endothelial growth factor A; HCAECs, human coronary artery endothelial cells; qRT-PCR, quantitative reverse transcription polymerase chain reaction.

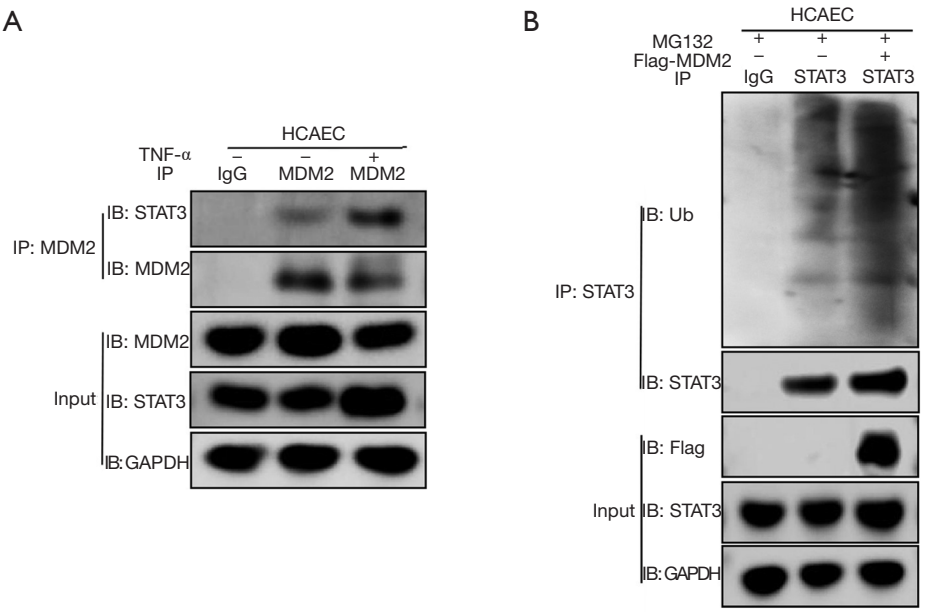

Figure 5 MDM2 can act as an E3 ligase of STAT3. (A) HCAECs were treated with TNF-α (40 ng/mL) for 4 h. STAT3 was immunoprecipitated. The input protein was immunoblotted with antibodies against MDM2 and GAPDH. (B) LV-Flag-MDM2 lentiviruses were transfected into HCAECs, and STAT3 ubiquitination increased significantly when the cells were treated for 6 h with the proteasome inhibitor MG132 (20 μM) 72 h after transfection. TNF-α, tumor necrosis factor α; IgG, immunoglobulin G; HCAECs, human coronary artery endothelial cells; MDM2, murine double minute 2; STAT3, signal transducer and activator of transcription 3.

damage, which is also an important risk factor for ischemic heart attack in adulthood (28). The coronary artery is a common invasive site of KD, that can cause destruction, dilatation, rupture, stenosis, and even embolism of the vascular wall (29). During coronary artery damage, vascular stability plays a key role. Vascular stability is closely related to the vascular endothelium. Abnormal functions of vascular endothelial cells can lead to hemodynamic abnormalities, blood hypercoagulability, and thrombosis, which are the main characteristics of KD (30). Inflammatory factors highly expressed in peripheral blood in acute KD patients are related to the proliferation and migration of endothelial cells and are involved in the occurrence and development of KD vasculitis (31).

The MDM2 protein is expressed in many human organs, such as vascular endothelial cells, T cells, vascular smooth muscle cells, skeletal muscle cells, and tumor cells (32). It is involved in various physiological and pathological processes of cells, including the cell cycle, apoptosis, tumorigenesis, metastasis, and angiogenesis. An imbalance in the expression of MDM2 is related to cardiovascular injury (33). The inhibition of MDM2 in atherosclerosis can reverse the damage to the vascular endothelium caused by oxidative stress (34). MDM2 can also activate nuclear factor kappa B (NF-κB), which causes the release of many inflammatory cytokines and leads to cardiac insufficiency and myocardial fibrosis (35). In the heart tissue of patients with ischemic cardiomyopathy and idiopathic dilated cardiomyopathy, the level of MDM2 mRNA is significantly downregulated. The downregulation of MDM2 can activate p53, which can promote the apoptosis of cardiomyocytes (36). The overexpression of MDM2 can inhibit the decrease in the rate of endothelial cell proliferation and the increase in the rate of apoptosis in coronary atherosclerosis (37). Additionally, MDM2 dynamically regulates the protein stability of both hypoxia-inducible factor 1 alpha (HIF1α) and hypoxia-inducible factor 2 alpha (HIF2α)/endothelial PAS domain protein 1 (EPAS1) through canonical and noncanonical mechanisms. The resulting HIF imbalance leads to reduced proangiogenic gene expression during a key period of myocardial capillary growth (38). These results together suggest that MDM2 is involved in cardiovascular diseases.

We found that the level of MDM2 mRNA expression in PBMCs from acute KD patients was significantly lower than that in PBMCs from patients in the fever and normal

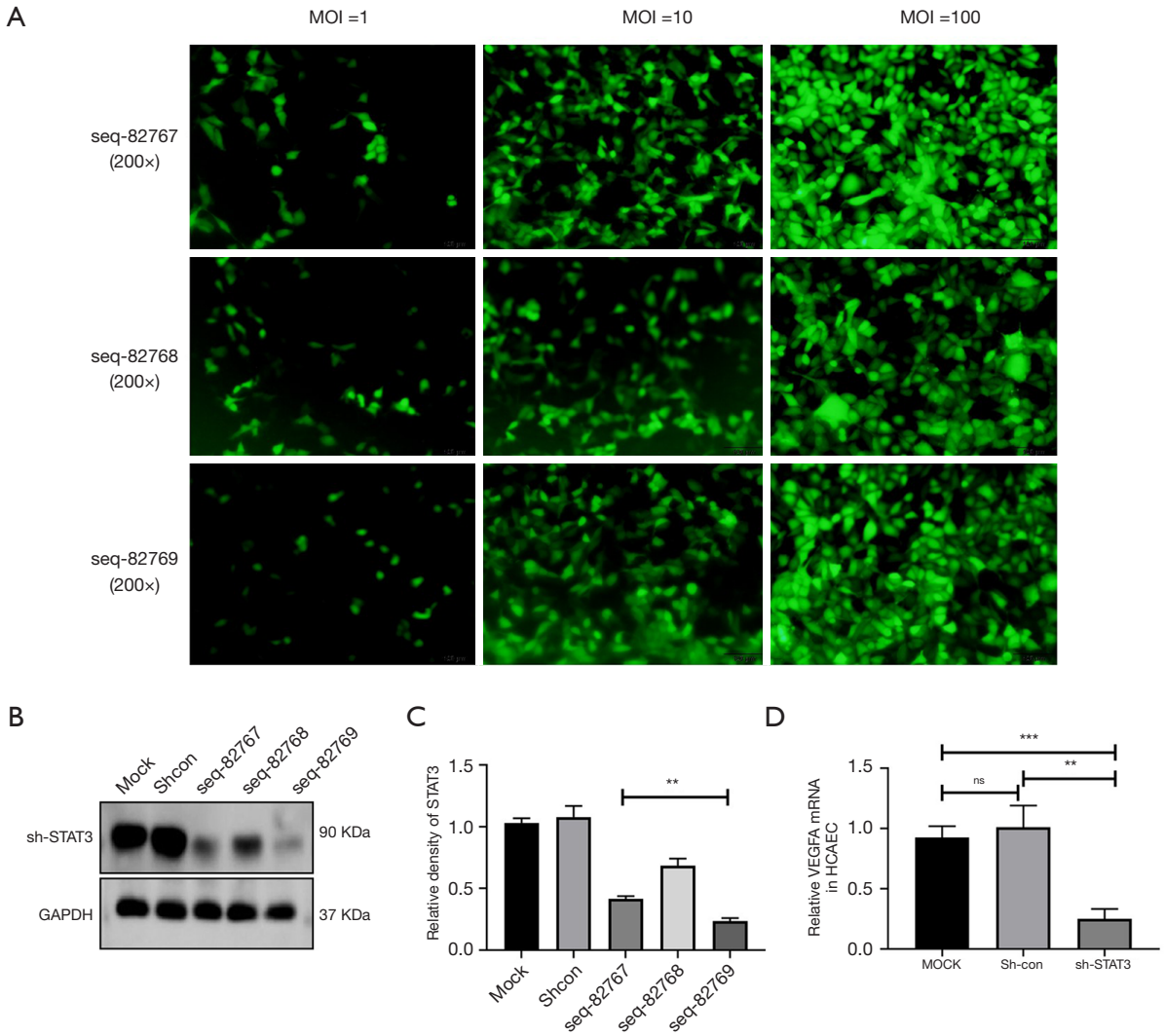

Figure 6 STAT3 regulated VEGFA *in vitro*. (A) The lentivirus used to downregulate *STAT3* (sh-STAT3) was transfected into HCAECs at MOIs of 1, 10, and 100 at 72 h after transfection. The fluorescence intensity of the cells was observed under a fluorescence microscope (green fluorescent protein marker). (B) Western blotting analysis was performed for STAT3 after the transfection of viruses carrying three different shRNA sequences into HCAECs to interfere with the expression of *STAT3*. (C) Image J software was used to analyze the effects of the three different STAT3-interfering viruses (sh-STAT3) on STAT3 protein levels. (D) qRT-PCR analysis was performed to determine the *VEGFA* mRNA levels in HCAECs transfected with STAT3-interfering viruses (sh-STAT3). ***, P<0.001; **, P<0.01; ns, no significance. MOI, multiplicity of infection; STAT3, signal transducer and activator of transcription 3; HCAECs, human coronary artery endothelial cells; VEGFA, vascular endothelial growth factor A; qRT-PCR, quantitative reverse transcription polymerase chain reaction.

groups (*Figure 1B*). Additionally, the level of MDM2 protein in mouse heart tissue decreased. These results indicated that MDM2 plays a role in the pathological and physiological changes in patients with KD.

The MDM2 protein is an important E3 ubiquitin ligase and is mainly found in the nucleus, where it regulates and degrades related proteins through the ubiquitin-proteasome system (39). By using UbiBrowser (http://ubibrowser.bio-it.cn/ubibrowser_v3/) and a human ubiquitin ligase-substrate interaction prediction and display system, we found that STAT3 was a predicted substrate of MDM2. STAT3 is a member of the STAT family and can control the development, proliferation, and differentiation of different types of cells, maintain the stability of the internal

environment, participate in the proliferation and apoptosis of cells, regulate angiogenesis and immune response, and influence the transduction of effector proteins and activation of transcription (40).

To further investigate the relationship between MDM2 and STAT3, we simulated the vascular inflammatory damage model of KD *in vitro* and found that the expression of MDM2 decreased while the expression of STAT3 increased in endothelial cells, which was similar to the results obtained from human PBMCs and mouse models. In this vascular endothelial inflammatory cell model, observations under a confocal microscope showed a significant increase in the number of cells with colocalized MDM2 and STAT3, especially in the nucleus. We also constructed *MDM2* overexpression/knockdown HCAECs via lentiviral transfection and found that the STAT3 level changed significantly; *MDM2* knockout increased the STAT3 level, whereas *MDM2* overexpression decreased the STAT3 level. This finding implied an interaction between MDM2 and STAT3. To verify that MDM2 can interact with STAT3, we treated HCAECs with TNFα. Our findings showed that MDM2 coimmunoprecipitated with STAT3.

The activation of STAT3 can inhibit T-cell apoptosis in the acute phase of KD. Activated T cells release many inflammatory cytokines into the blood, and these cytokines participate in the pathogenesis of KD (11). The activation of STAT3 can promote the activation and transcription of VEGF (41,42). The upregulation of STAT3 can increase the expression of Th17/Tregs. Tregs can secrete a large quantity of VEGFA. The promoter of the *VEGFA* gene lacks a Treg-specific transcription factor forkhead box P3 (FOXP3) binding site. FOXP3 along with the locus-specific transcription factor STAT3 was found to bind to the *VEGF*A promoter to induce its transcription in Treg cells obtained from breast cancer patients (43-45). Additionally, the activation of STAT3 can regulate VEGFA to increase vascular permeability (46).

The VEGFA protein can act as a regulator of angiogenesis and participate in angiogenesis, endothelial cell survival, and the regulation of vascular permeability (47). An increase in plasma VEGFA levels in children with KD complicated with CAL can cause changes in vascular permeability, which is closely related to the injury of the vascular endothelium in children with KD VEGFA and is an important factor associated with KD complicated with CAL (48-50).

We also showed that STAT3 can regulate the transcription of *VEGFA*. The level of STAT3 in PBMCs and the level of VEGFA in plasma were higher in children with KD in the acute stage, and the levels of the STAT3 protein and *VEGFA* mRNA were significantly higher in mouse heart tissue. The expression of *VEGFA* mRNA also decreased significantly when *STAT3* was knocked down in HCAECs via lentivirus transfection.

CALs in KD are a chronic problem, and abnormalities in the structure or function of the coronary artery occur even in the convalescent period (51,52). In our study, the levels of STAT3 in PBMCs and VEGFA in the plasma of children with KD decreased significantly after treatment, but they were still higher than those in the normal and fever groups. Based on our results and the findings of other studies, we first elucidated the relationship between MDM2 and STAT3 in the pathogenesis of KD, in which, MDM2 ubiquitin was found to modify its substrate protein STAT3. Therefore, we speculated that the downregulation of MDM2 in the acute stage of KD can induce a reduction in ubiquitin-mediated degradation of STAT3, which in turn can lead to the upregulation of VEGFA. These changes might be associated with the pathogenesis of KD.

Conclusions

Our study identified MDM2 as a negative regulator of STAT3 signaling by regulating its ubiquitination during inflammatory responses in KD, and demonstrated that it might serve as a candidate therapeutic target for KD.

Acknowledgments

We are grateful to the Institute of Pediatric Research, Children's Hospital of Soochow University, for their provision of the equipment necessary to carry out the study. We appreciate its support for this study.

Funding: This project was funded by the National Natural Science Foundation of China (Nos. 81970436, 82171797, 82371806, 81971477, 81870365, 82070512), the National Science Foundation for Youths of China (Nos. 81800437 and 81900450), the Jiangsu Provincial Social Development Project (No. SBE2021750252), the Applied Foundational Research of Medical and Health Care of Suzhou City (Nos. SYS2019086, SKYD2022137), and the Gusu Health Talent Program (No. GSWS2020038).

Footnote

Reporting Checklist: The authors have completed the MDAR

and ARRIVE reporting checklists. Available at https://tp.amegroups.com/article/view/10.21037/tp-23-459/rc

Data Sharing Statement: Available at https://tp.amegroups.com/article/view/10.21037/tp-23-459/dss

Peer Review File: Available at https://tp.amegroups.com/article/view/10.21037/tp-23-459/prf

Conflicts of Interest: All authors have completed the ICMJE uniform disclosure form (available at https://tp.amegroups.com/article/view/10.21037/tp-23-459/coif). The authors have no conflicts of interest to declare.

Ethical Statement: The authors are accountable for all aspects of the work in ensuring that questions related to the accuracy or integrity of any part of the work are appropriately investigated and resolved. The clinical study was approved by the Ethics Committee of the Children's Hospital of Soochow University (reference number 2021CS013) and was conducted in compliance with the Declaration of Helsinki (as revised in 2013). The Ethics Committee informed all the participants and their parents about the study details, who then provided written informed consent. The animal experiments were conducted following the National Institutes of Health Guide for the Care and Use of Laboratory Animals. The Animal Care and Use Committee of Soochow University approved the experiments (approval number: SUDA20220906A01).

References

1. Dietz SM, van Stijn D, Burgner D, et al. Dissecting Kawasaki disease: a state-of-the-art review. Eur J Pediatr 2017;176:995-1009.
2. Pilania RK, Bhattarai D, Singh S. Controversies in diagnosis and management of Kawasaki disease. World J Clin Pediatr 2018;7:27-35.
3. Wang Y, Li T. Advances in understanding Kawasaki disease-related immuno-inflammatory response and vascular endothelial dysfunction. Pediatr Investig 2022;6:271-9.
4. Anzai F, Watanabe S, Kimura H, et al. Crucial role of NLRP3 inflammasome in a murine model of Kawasaki disease. J Mol Cell Cardiol 2020;138:185-96.
5. Swanson KV, Deng M, Ting JP. The NLRP3 inflammasome: molecular activation and regulation to therapeutics. Nat Rev Immunol 2019;19:477-89.
6. Majolée J, Kovačević I, Hordijk PL. Ubiquitin-based modifications in endothelial cell-cell contact and inflammation. J Cell Sci 2019;132:jcs227728.
7. Zou Q, Jin J, Hu H, et al. USP15 stabilizes MDM2 to mediate cancer-cell survival and inhibit antitumor T cell responses. Nat Immunol 2014;15:562-70.
8. Zafar A, Khan MJ, Naeem A. MDM2- an indispensable player in tumorigenesis. Mol Biol Rep 2023;50:6871-83.
9. Lin TC, Lin CS, Tsai TN, et al. Stimulatory Influences of Far Infrared Therapy on the Transcriptome and Genetic Networks of Endothelial Progenitor Cells Receiving High Glucose Treatment. Acta Cardiol Sin 2015;31:414-28.
10. Lv YW, Chen Y, Lv HT, et al. Kawasaki disease OX40-OX40L axis acts as an upstream regulator of NFAT signaling pathway. Pediatr Res 2019;85:835-40.
11. Wang X, Ding YY, Chen Y, et al. Corrigendum: MiR-223-3p Alleviates Vascular Endothelial Injury by Targeting IL6ST in Kawasaki Disease. Front Pediatr 2019;7:449.
12. Ji Z, He L, Regev A, et al. Inflammatory regulatory network mediated by the joint action of NF-kB, STAT3, and AP-1 factors is involved in many human cancers. Proc Natl Acad Sci U S A 2019;116:9453-62.
13. Fan D, Jiang WL, Jin ZL, et al. Leucine zipper protein 1 attenuates pressure overload-induced cardiac hypertrophy through inhibiting Stat3 signaling. J Adv Res 2023;S2090-1232(23)00299-0.
14. Zhao M, Gao FH, Wang JY, et al. JAK2/STAT3 signaling pathway activation mediates tumor angiogenesis by upregulation of VEGF and bFGF in non-small-cell lung cancer. Lung Cancer 2011;73:366-74.
15. Wu X, Deng Y, Zu Y, et al. Erratum: Histone demethylase KDM4C activates HIF1α/VEGFA signaling through the costimulatory factor STAT3 in NSCLC. Am J Cancer Res 2022;12:5692-3.
16. Yu H, Lee H, Herrmann A, et al. Revisiting STAT3 signalling in cancer: new and unexpected biological functions. Nat Rev Cancer 2014;14:736-46.
17. Wang Z, Yan M, Li J, et al. Dual functions of STAT3 in

LPS-induced angiogenesis of hepatocellular carcinoma. Biochim Biophys Acta Mol Cell Res 2019;1866:566-74.
18. Owen KL, Brockwell NK, Parker BS. JAK-STAT Signaling: A Double-Edged Sword of Immune Regulation and Cancer Progression. Cancers (Basel) 2019;11:2002.
19. Yuan ZL, Guan YJ, Chatterjee D, et al. Stat3 dimerization regulated by reversible acetylation of a single lysine residue. Science 2005;307:269-73.
20. Wang R, Cherukuri P, Luo J. Activation of Stat3 sequence-specific DNA binding and transcription by p300/CREB-binding protein-mediated acetylation. J Biol Chem 2005;280:11528-34.
21. Fan X, Shan X, Jiang S, et al. YAP promotes endothelial barrier repair by repressing STAT3/VEGF signaling. Life Sci 2020;256:117884.
22. Huang J, Zhang S. Overexpressed Neuropilin-1 in Endothelial Cells Promotes Endothelial Permeability through Interaction with ANGPTL4 and VEGF in Kawasaki Disease. Mediators Inflamm 2021;2021:9914071.
23. Saito K, Nakaoka H, Takasaki I, et al. MicroRNA-93 may control vascular endothelial growth factor A in circulating peripheral blood mononuclear cells in acute Kawasaki disease. Pediatr Res 2016;80:425-32.
24. Chen CY, Huang SH, Chien KJ, et al. Reappraisal of VEGF in the Pathogenesis of Kawasaki Disease. Children (Basel) 2022;9:1343.
25. McCrindle BW, Rowley AH, Newburger JW, et al. Diagnosis, Treatment, and Long-Term Management of Kawasaki Disease: A Scientific Statement for Health Professionals From the American Heart Association. Circulation 2017;135:e927-99.
26. Huang H, Dong J, Jiang J, et al. The role of FOXO4/NFAT2 signaling pathway in dysfunction of human coronary endothelial cells and inflammatory infiltration of vasculitis in Kawasaki disease. Front Immunol 2022;13:1090056.
27. Livak KJ, Schmittgen TD. Analysis of relative gene expression data using real-time quantitative PCR and the 2(-Delta Delta C(T)) Method. Methods 2001;25:402-8.
28. Kuo HC. Diagnosis, Progress, and Treatment Update of Kawasaki Disease. Int J Mol Sci 2023;24:13948.
29. Yonesaka S, Takahashi T, Eto S, et al. Biopsy-proven myocardial sequels in Kawasaki disease with giant coronary aneurysms. Cardiol Young 2010;20:602-9.
30. Tsuda E, Tsujii N, Hayama Y. Stenotic Lesions and the Maximum Diameter of Coronary Artery Aneurysms in Kawasaki Disease. J Pediatr 2018;194:165-170.e2.
31. Wojdasiewicz P, Wajda A, Haładyj E, et al. IL-35, TNF-α, BAFF, and VEGF serum levels in patients with different rheumatic diseases. Reumatologia 2019;57:145-50.
32. Jean-Charles PY, Yu SM, Abraham D, et al. Mdm2 regulates cardiac contractility by inhibiting GRK2-mediated desensitization of β-adrenergic receptor signaling. JCI Insight 2017;2:e95998.
33. Shen H, Zhang J, Wang C, et al. MDM2-Mediated Ubiquitination of Angiotensin-Converting Enzyme 2 Contributes to the Development of Pulmonary Arterial Hypertension. Circulation 2020;142:1190-204.
34. Zeng Y, Xu J, Hua YQ, et al. MDM2 contributes to oxidized low-density lipoprotein-induced inflammation through modulation of mitochondrial damage in endothelial cells. Atherosclerosis 2020;305:1-9.
35. Zhao H, Shen R, Dong X, et al. Murine Double Minute-2 Inhibition Attenuates Cardiac Dysfunction and Fibrosis by Modulating NF-κB Pathway After Experimental Myocardial Infarction. Inflammation 2017;40:232-9.
36. Hauck L, Stanley-Hasnain S, Fung A, et al. Cardiac-specific ablation of the E3 ubiquitin ligase Mdm2 leads to oxidative stress, broad mitochondrial deficiency and early death. PLoS One 2017;12:e0189861.
37. Zhang H, Zhang S, Yu M, et al. MDM2 gene inhibited lPS-induced decrease in proliferation rate and increase in apoptosis rate of human umbilical vein endothelial cells. Chinese Journal of Immunology 2019;35:1553-8.
38. Shridhar P, Glennon MS, Pal S, et al. MDM2 Regulation of HIF Signaling Causes Microvascular Dysfunction in Hypertrophic Cardiomyopathy. Circulation 2023;148:1870-86.
39. Brockhaus K, Böhm MRR, Melkonyan H, et al. Age-related Beta-synuclein Alters the p53/Mdm2 Pathway and Induces the Apoptosis of Brain Microvascular Endothelial Cells In Vitro. Cell Transplant 2018;27:796-813.
40. Dong Y, Chen J, Chen Y, et al. Targeting the STAT3 oncogenic pathway: Cancer immunotherapy and drug repurposing. Biomed Pharmacother 2023;167:115513.
41. Sun X, Lu Y, Lei T. Correction to: TPTEP1 suppresses high glucose induced dysfunction in retinal vascular endothelial cells by interacting with STAT3 and targeting VEGFA. Acta Diabetol 2023;60:143-5.
42. Ma X, Ning S. Cyanidin-3-glucoside attenuates the angiogenesis of breast cancer via inhibiting STAT3/VEGF pathway. Phytother Res 2019;33:81-9.
43. Yang XO, Panopoulos AD, Nurieva R, et al. STAT3 regulates cytokine-mediated generation of inflammatory helper T cells. J Biol Chem 2007;282:9358-63.
44. Lv J, Sun B, Mai Z, et al. STAT3 potentiates the ability

of airway smooth muscle cells to promote angiogenesis by regulating VEGF signalling. Exp Physiol 2017;102:598-606.
45. Kajal K, Bose S, Panda AK, et al. Transcriptional regulation of VEGFA expression in T-regulatory cells from breast cancer patients. Cancer Immunol Immunother 2021;70:1877-91.
46. Wang L, Astone M, Alam SK, et al. Suppressing STAT3 activity protects the endothelial barrier from VEGF-mediated vascular permeability. Dis Model Mech 2021;14:dmm049029.
47. Pérez-Gutiérrez L, Ferrara N. Biology and therapeutic targeting of vascular endothelial growth factor A. Nat Rev Mol Cell Biol 2023;24:816-34.
48. Miura M, Garcia FL, Crawford SE, et al. Cell adhesion molecule expression in coronary artery aneurysms in acute Kawasaki disease. Pediatr Infect Dis J 2004;23:931-6.
49. Breunis WB, Davila S, Shimizu C, et al. Disruption of vascular homeostasis in patients with Kawasaki disease: involvement of vascular endothelial growth factor and angiopoietins. Arthritis Rheum 2012;64:306-15.
50. Zhou Y, Wang S, Zhao J, et al. Correlations of complication with coronary arterial lesion with VEGF, PLT, D-dimer and inflammatory factor in child patients with Kawasaki disease. Eur Rev Med Pharmacol Sci 2018;22:5121-6.
51. Zhang D, Liu L, Huang X, et al. Insights Into Coronary Artery Lesions in Kawasaki Disease. Front Pediatr 2020;8:493.
52. Gong X, Tang L, Wu M, et al. Development of a nomogram prediction model for early identification of persistent coronary artery aneurysms in kawasaki disease. BMC Pediatr 2023;23:79.

Cite this article as: Xu L, Qian GH, Zhu L, Huang HB, Huang CC, Qin J, Zheng YM, Sun L, Ren Y, Ding YY, Lv HT. Ubiquitin ligase MDM2 mediates endothelial inflammation in Kawasaki disease vasculitis development. Transl Pediatr 2024;13(2):271-287. doi: 10.21037/tp-23-459